8th International Conference on Seismology & Earthquake Engineering
11-13 Nov. 2019, Tehran, Iran

3D VELOCITY MODEL OF CRUST BENEATH THE ZAGROS COLLISION ZONE FROM AMBIENT NOISE TOMOGRAPHY

Zahra ZARUNIZADEH
Ph.D. Student, Department of Earth Sciences, Institute for Advanced Studies in Basic Sciences, Zanjan, Iran
z.zarunizadeh@iasbs.ac.ir

Khalil MOTAGHI
Assistant Professor, Department of Earth Sciences, Institute for Advanced Studies in Basic Sciences, Zanjan, Iran
kmotaghi@iasbs.ac.ir

Abdelkrim AOUDIA
Research Scientist, International Centre for Theoretical Physics, Trieste, Italy
aoudia@ictp.it

Surya PACHHAI
Researcher, Institute of Geophysics and Planetary Physics, Scripps Institution of Oceanography, University of California, San Diego, California, USA
spachhai@ucsd.edu

Wathiq ABDULNABY
Researcher, Department of Geology, University of Basrah, Basrah, Iraq
wgabdulnaby@ualr.edu

Abdolreza GHODS
Associate Professor, Institute for Advanced Studies in Basic Sciences, Zanjan, Iran
aghods@iasbs.ac.ir

Keywords: Ambient noise tomography, Cross correlation, Bayesian Monte-Carlo, Crustal structure, Zagros collision zone

Zagros collision zone was formed by collision between the Arabian plate and central Iranian micro-continent. The Zagros belt is important in terms of one of the youngest and most active continental collisions while interactions with its deformation zone continues. In order to study the crustal structure across the northern part of the Zagros collision zone, we process continuous vertical-component seismograms recorded by ~85 broad-band stations situated in the east of Iraq, Zagros Mountains, Central Iran and western Alborz (Figure 1-a). To estimate the inter-station Green functions by cross-correlation, we employed a method described by Bensen et al. (2007). A multiple-filter analysis technique (e.g., Dziewonski et al., 1969) was employed to visually determine both the group and phase velocities of fundamental mode Rayleigh waves between periods of 5 and 35 s. To construct the phase and group velocity maps, we used the two-dimensional technique developed by Ditmar and Yanovskaya (1987). The phase and group velocity maps with a lateral resolution of ~ 60 km for most of the study region were generated. To constructed 1-D velocity model to Rayleigh phase and group dispersion curves, a Bayesian Monte-Carlo algorithm (Manu-Marfo et al., 2019) was applied on $0.3^\circ \times 0.3^\circ$ geographic grids. Juxtaposing the all shallow 1D models generated by inversion of noise tomographies, we composed a 3D velocity model for the study region which is the first high resolution crustal image beneath the Zagros collision zone. 3-D model reveals a shallow (< 15 km) low velocity anomaly beneath the Zagros Mountains (Figure 2) consistent with the geology. It is almost known that the Zagros was covered by a thick sedimentary layer (~ 10 km). Similar shallow low velocity anomaly is observed beneath Central Iran in section A-A' (Figure 2-a) where thick sedimentary layer was reported before by geology (Teknik and Ghods, 2017). The shallow high velocity anomaly is a continuous suture-parallel feature observable beneath the most of the SSZ as it is shown in the vertical sections A-A' and B-B' (Figure 2). The most prominent shallow feature observed in the 3D velocity model is the mid-crustal low velocity (Vs ~ 3.2 km/s) layer beneath the Zagros Mountains at depth between 20 km and 30 km. This low velocity layer looks like the mid-crustal low velocity layer beneath Tibetan plateau (Klemperer, 2006 and references therein) generated by a crustal channel flow.

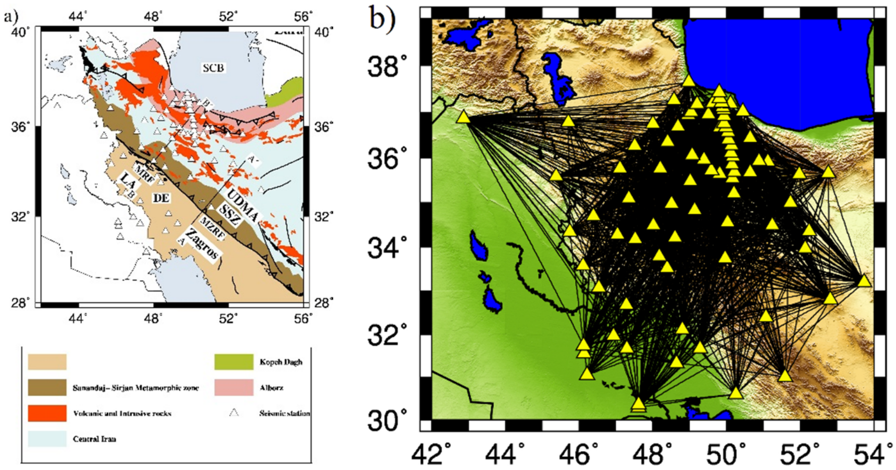

Figure 1. a): Geological map of study region illustrating the locations of major tectonic structures: Zagros, Sanandaj-Sirjan metamorphic zone (SSZ), Urmia-Dokhtar magmatic arc (UDMA), South Caspian Basin (SCB), Alborz, Kopeh Dagh and Central Iran. The black solid lines represent active faults. Triangles show location of seismic stations. MZF: Main Zagros Fault, MZRF: Main Zagros Reverse Fault, LA: Lurestan Arc, DE: Dezful embracement. AA' and BB' are location of two vertical cross-section in (Figure 2). b): Inter-station paths for all the group and phase speed measurements.

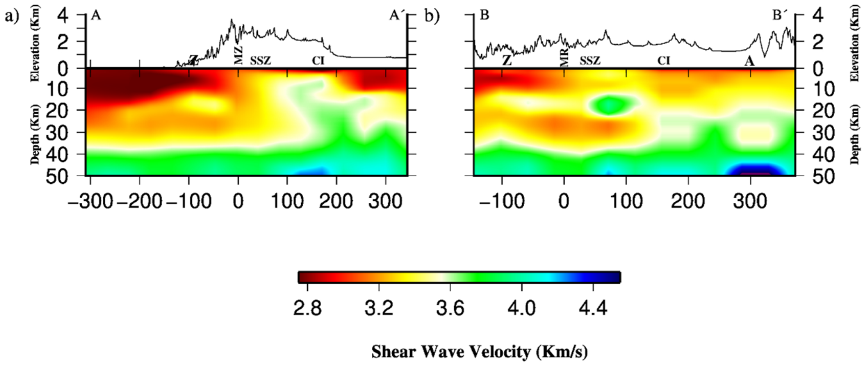

Figure 2. Vertical cross sections of shear wave velocity along two profiles. The locations of the profiles are plotted in (Figure 1-a). Topography is shown in above panels.

REFERENCES

Bensen, G.D., Ritzwoller, M.H., Barmin, M.P., Levshin, A.L., Lin, F., Moschetti, M.P., Shapiro, N. M., and Yang, Y. (2007). Recessing seismic ambient noise data to obtain reliable broad-band surface wave dispersion measurements. *Geophys. J. Int.*, *169*, 1239-1260.

Ditmar, P.G. and Yanovskaya, T.B. (1987). *A Generalization of the Backus-Gilbert Method for Estimation of Lateral Variations of Surface Wave Velocity. Izv. Akad. Nauk SSSR, Fiz. Zeml*, *6*, 30–60 (in Russian).

Dziewonski, A., Bloch, S., and Landisman, M. (1969). A technique for the analysis of transient seismic signals. *Bull. Seismol. Soc. Am.*, *59*, 427-444.

Klemperer, S.L. (2006). Crustal flow in Tibet: geophysical evidence for the physical state of Tibetan lithosphere, and inferred patterns of active flow. *Geological Society, London, Special Publications*, 268, 39-70.

Manu-Marfo, D., Aoudia, A., Pachhai, S., and Kherchouche, R. (2019). *3D shear wave velocity model of the crust and uppermost mantle beneath the Tyrrhenian basin and margins.* Scientific reports, *9*(1), 3609.

Teknik, V. and Ghods, A. (2017). Depth of magnetic basement in Iran based on fractal spectral analysis of aeromagnetic data. *Geophys. J. Int.*, *209*, 1878-1891.